Separation Science and Technology
Publication details, including instructions for authors and subscription information:
http://www.informaworld.com/smpp/title~content=t713708471

The Vibrating Ultrafiltration Module. Performance in the Low Frequency Region

F. Vigo[a]; C. Uliana[a]; E. Ravina[b]
[a] INSTITUTE OF INDUSTRIAL CHEMISTRY UNIVERSITY OF GENOA, GENOA, ITALY [b] INSTITUTE OF APPLIED MECHANICS UNIVERSITY OF GENOA, GENOA, ITALY

To cite this Article Vigo, F. , Uliana, C. and Ravina, E.(1990) 'The Vibrating Ultrafiltration Module. Performance in the Low Frequency Region', Separation Science and Technology, 25: 1, 63 — 82
To link to this Article: DOI: 10.1080/01496399008050321
URL: http://dx.doi.org/10.1080/01496399008050321

SEPARATION SCIENCE AND TECHNOLOGY, 25(1 & 2), pp. 63-82, 1990

The Vibrating Ultrafiltration Module. Performance in the Low Frequency Region

F. VIGO and C. ULIANA

INSTITUTE OF INDUSTRIAL CHEMISTRY
UNIVERSITY OF GENOA
16132, GENOA, ITALY

E. RAVINA

INSTITUTE OF APPLIED MECHANICS
UNIVERSITY OF GENOA
16145, GENOA, ITALY

Abstract

The effect of vibrations on oil emulsion ultrafiltration was studied as a function of frequency (in the 0-50 Hz range) and of amplitude (0.0016-0.045 m). The experimental date obtained show that a minimal ("critical") frequency must be reached in order to achieve effective ultrafiltration of oil from water. This "critical" frequency depends only on vibration amplitude. It was also found that the permeate flux increases with frequency and reaches a plateau value which depends only on the applied pressure. A mathematical relation is proposed in order to relate these parameters and to predict the behavior of the vibrating module in conditions different from the experimental ones. The energy consumption of such a module was evaluated as a function of the operative variables in order to determine the optimal working conditions.

INTRODUCTION

The ultrafiltration (UF) process is increasingly applied by industry for separation or pollution abatement purposes (*1*). The choice of this technique is suggested for both technical and economic reasons. The latter reason may sometimes advise against its application as, for example, in the case of pollution control which normally is not a pay-back process.

UF still has some drawbacks limiting its feasibility: cost of membranes, poor performance connected with membrane fouling and damage, and energy losses connected with the need to recycle large volumes over the membranes.

The cost of membranes and their properties are a concern of chemists. Studies still in progress have produced promising results (*2*).

The efficiency of a membrane, the energy consumption, and the size of the treated volumes are directly related to the type of module and its hydrodynamic conditions.

In previous work (*3, 4*) we demonstrated that nonconventional modules can be used in the UF process with appreciable advantages. In particular, we studied the performances of rotating modules with the aim of reducing both the volumes involved and the energy losses. The good results we obtained were ascribed to the formation of "Taylor vortexes" (*5*) able to destroy the boundary layer (*6*) which is responsible for UF efficiency reduction and membrane fouling.

The "Taylor vortexes" are typical of fluids subjected to cylindrical motion (Couette motion) and cause a very efficient mass exchange, preventing the build-up of concentrated layers on the surface of the membrane (*7*). They have a similar effect on the heat exchange coefficient (*8*), and it is also reported (*9–12*) that the vibrations can do the same thing.

The effect of vibrations on the mass transfer coefficient during membrane processes has been both studied and applied. Acoustical vibrations have been used to improving performance in separation processes involving membranes (*13*). In some cases the vibrations were applied to the membrane by means of an electromagnetic coupling (*14, 15*), while pulsating flows were employed at other times (*16*).

Our intent was to explore a range of low frequency vibrations (0–50 Hz), tangentially applied to the membrane surface by means of a mechanical coupling, with the aim of creating a new type of device useful for practical application in the UF processes.

EXPERIMENTAL

Ultrafiltration Module

We used the membrane permeator described in earlier papers (*3, 4*). It consisted of a drum carrying a Celgard 3500 membrane and moving in a cylindrical shell of 0.005 m diameter. The membrane area was 0.07 m^2.

This modlule was connected with a mechanical device which forced it to move in a reciprocating motion.

The purposes of our study required the application of a periodically oscillating motion to the membrane axis. The choice of the drive depended on several factors (the fluctuation of the acceleration value and the related inertial forces with frequency and amplitude, system balancing problems) which prevented the application of some theoretically suitable solutions (for instance, cam and spring, linkages).

We adopted the face cam-follower device as the best compromise between performance and ease of execution. We took great care to limit friction at the contact points.

The apparatus was driven by a 560-W dc electric motor. The frequency of the oscillations could be varied continuously from 0 to 50 Hz, while the amplitude was determined by mechanical adjustments to the device reported in Fig. 1. Amplitudes (at the membrane surface) of 0.0016, 0.0032, 0.01, and 0.045 m were tested.

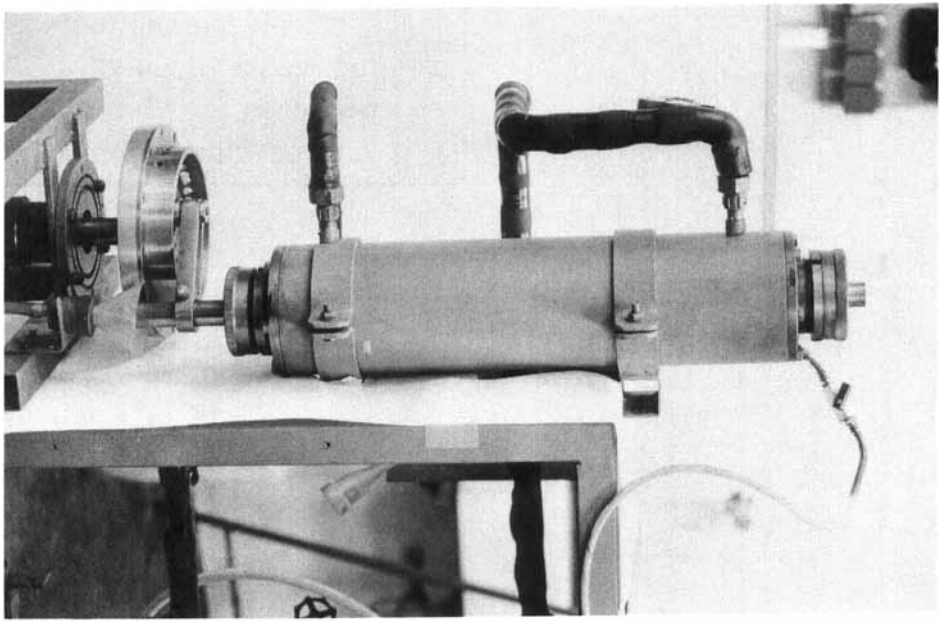

FIG. 1. Experimental apparatus.

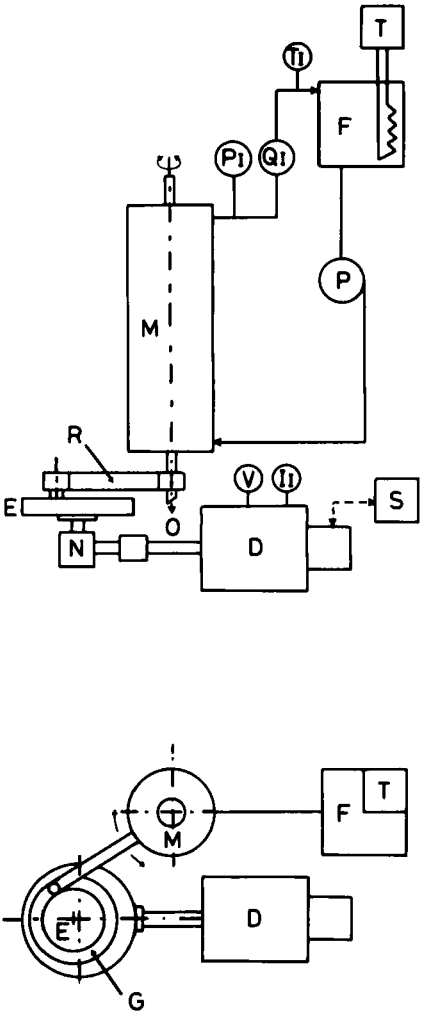

D	DRIVING MOTOR
E	FACE CAM WITH OSCILLATING FOLLOWER (POSITIVE MOTION)
F	FEED TANK
G	ECCENTRIC GROOVE
M	MODULE
N	STRAIGHT BEVEL GEARS
O	PERMEATE OUTLET
P	GEAR PUMP
P_I	PRESSURE GAUGE
Q_I	FLUX INDICATOR
R	CONNECTING ROD
S	SPEED METER AND CONTROL
T	THERMOSTATIC UNIT
T_I	THERMOMETER
V, I_I	VOLTAGE-CURRENT INDIC.

FIG. 1 (*continued*).

The UF circuit was fed with a 20% cutting oil/water emulsion by means of a gear pump which could operate up to 800 kPa. The temperature was kept at 313 K during all the experiments. The power consumption was checked by current-voltage measurements. The rejection of oil was measured by turbidimetry and periodically checked by infrared spectroscopy (*17*). The permeate flux was volumetrically metered. Both parameters were evaluated after a period of time sufficient to exclude further variations due to membrane conditioning.

RESULTS AND DISCUSSION

Influence of the Frequency

Rejections and permeate fluxes were measured as functions of the vibration frequency at 4 different vibration amplitudes. The experimental values were recorded both with increasing and decreasing frequencies. During these runs the pressure was kept constant at values ranging between 50 and 800 kPa. A set of plots similar to that reported in Fig. 2 was obtained.

The data were manipulated in order to determine what mathematical relation related the various parameters. The logarithmic plotting of permeate flux values, for example, those reported in Fig. 3, allowed us to determine two interesting quantities: H_c ("critical frequency"), which is the frequency value at which the permeate flux starts increasing with frequency, and a, the exponent value at which the frequency influences the permeate flux increase. The plot also showed that H_c is the same for all pressures, depending only on the amplitude (δ) value when the other parameters, such as temperature and oil concentration, are kept constant. The a value depends on pressure (P) but remains constant at a mean value close to 1 while varying the vibration frequency (F).

Analysis of the experimental plot in Fig. 2 allows identification of the H_0 value which represents the minimum or "optimal" frequency at which oil rejection reaches 99.9%. H_0 depends on the pressure and vibration amplitude, as will be shown later.

Finally, the F plots in Fig. 2 seem likely to converge to the same plateau in spite of different δ values. We called this limiting value $F\infty$ and noticed that it depends only on P.

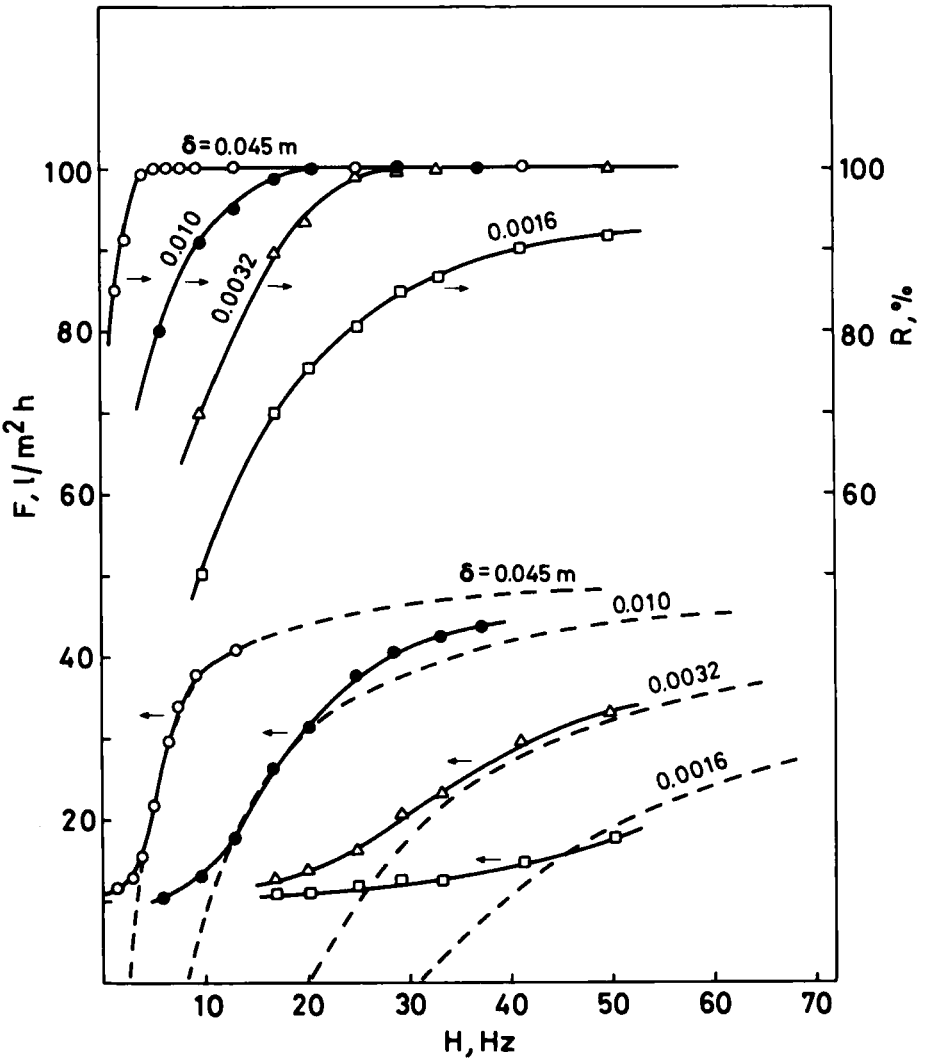

FIG. 2. Influence of the frequency H on the permeate flux F and the oil rejection R% at different vibration amplitudes (δ) and a pressure of 200 kPa. Full lines: experimental data. Dashed lines: calculated values.

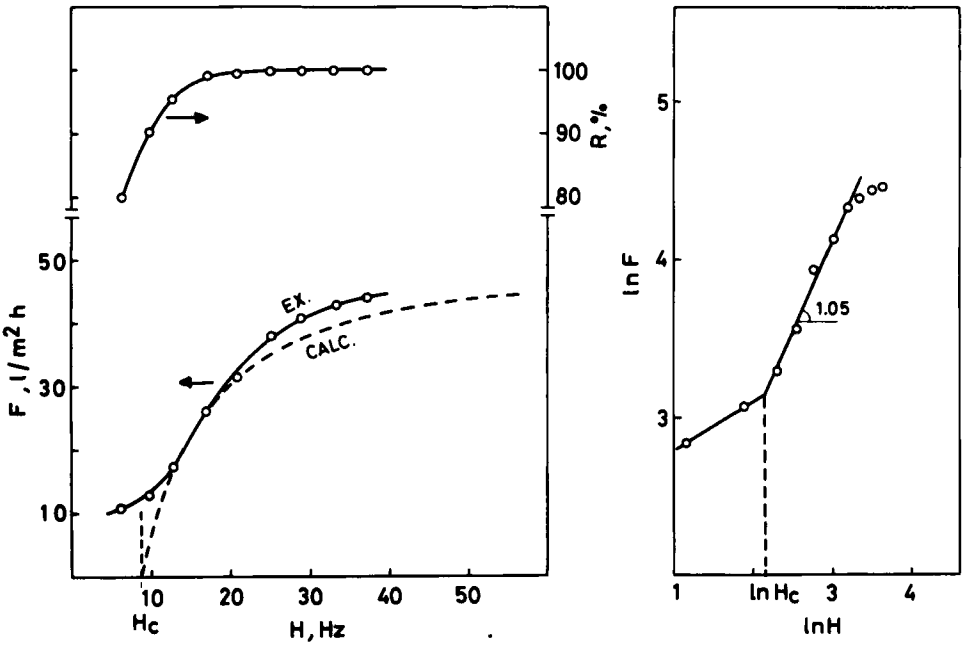

FIG. 3. Graphic evaluation of the "critical" frequency H_c and the exponent a in the case of δ = 0.010 m and 200 kPa pressure.

At first glance, these behaviors can be interpreted as follows: Before reaching the "critical" frequency, the polarization layer on the membrane (the so-called "boundary layer") hinders the permeation of water (the low values of flux measured in this region are attributed to the passing of the emulsion through the largest membrane pores). At H_c the boundary layer starts being destroyed, and both the flux and rejection increase.

A similar behavior was found in previous work concerning rotating modules (*3, 7*).

The "plateau" value $F\infty$, which depends on pressure (at constant temperature), is reasonably connected with the specific hydraulic head loss across the membrane and the aqueous phase viscosity. In other words, when a minimum thickness (ideally zero) of the boundary layer is reached, the permeate flux increase stops and only pressure enhancements can further affect it. The dependence of H_c and flux slope on δ is

probably due to speed fluctuation rather than to speed itself, as in the case of rotating modules (*3*). This can also be inferred from calculation of the average speed ($2H\delta$) which under no circumstances exceeded 1 m/s. A similar behavior was noted by Raben (*11*) for the heat transfer coefficient.

The following relation was then proposed in order to bind together the main parameters:

$$F(H) = kP^p\delta^d[1 - (1/H)]^a \quad (1)$$

where $F(H)$ = permeate flux F expressed as a function of H
H = vibration frequency (Hz)
P = pressure (kPa)
δ = vibration amplitude (m)

In order to check the fitness of Eq. (1), we tried to obtain the p and d exponents by measuring the experimental influence of pressure and vibration amplitude on F. The k value was evaluted both by analytical and iterative methods.

Influence of the Pressure

In Fig. 4 we report the permeate flux as a function of pressure as measured at three frequency values (5, 10, 15 Hz). The $H = \infty$ value was extrapolated. The experimental data indicate that the slope of the F/P plots (p exponent value) approaches the value 1, provided that a sufficiently high H value is reached. The following explanation is proposed: The pressure affects the permeate flux but acts both on water and oil. This means that the higher the pressure, the higher the flux. But this also applies to the contribution of oil accumulated on the membrane surface and the boundary layer thickness. Such a situation causes both the specific hydraulic permeability and the permeate flux limiting values to decrease, as can be observed in Fig. 4, if the frequency is not high enough.

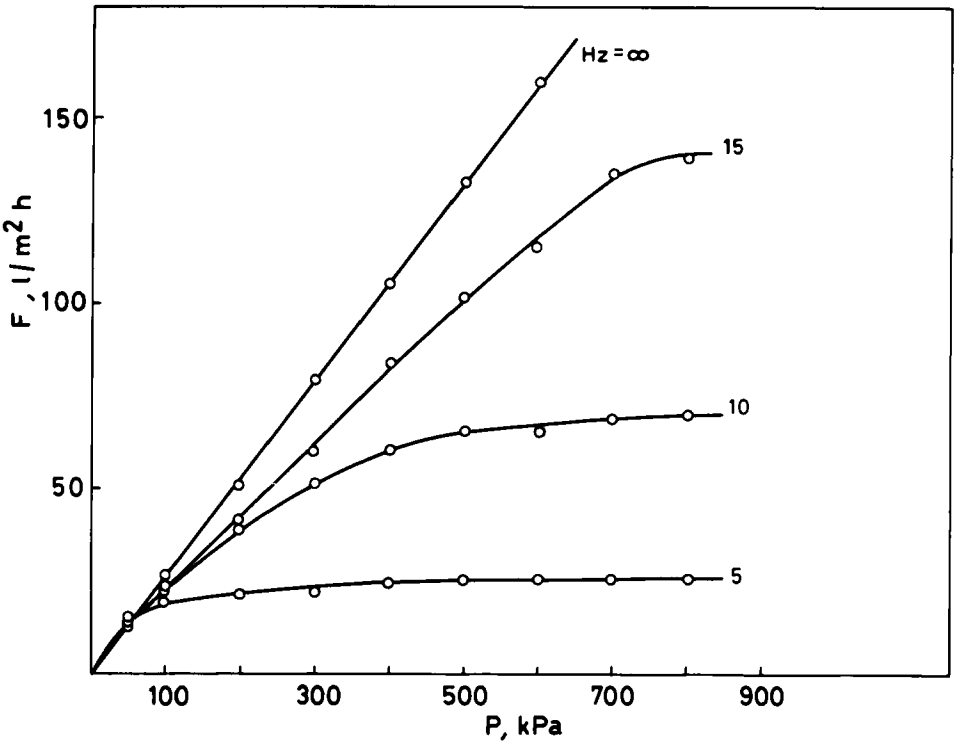

FIG. 4. Influence of the pressure P on the permeate flux F at different frequencies. δ = 0.045 m.

Vibration Amplitude

The vibration amplitude δ was varied by changing the cam schematized in Fig. 1, and the permeate flux was recorded at 4 δ values as a function of frequency.

The data already reported (Fig. 2) clearly show that the vibration amplitude affects the slopes of the plots (that is, the frequency necessary to have the same permeate flux). We therefore report in Fig. 5 the ratio F/H, calculated at three different F values (20, 25, 30 l m^{-2}/h), as a function of δ.

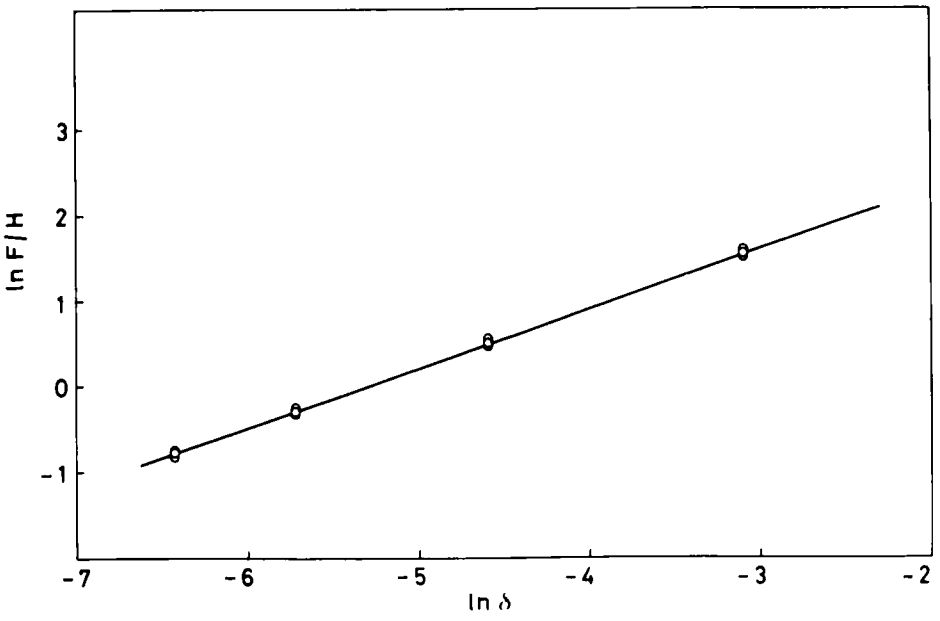

FIG. 5. The permeate flux/frequency ratio as a function of the amplitude δ. Pressure = 200 kPa.

Once more it was possible by logarithmic graphics to evaluate the δ exponent *d*. Values between 0.71 and 0.75 were found.

CHECK OF THE MATHEMATICAL MODEL

The experimental values obtained for the *a*, *p*, and *d* exponents were introduced into the proposed mathematical relation (Eq. 1). Their fitness was then checked by means of an iterative method (EUREKA software). The best fit was obtained for the expression

$$F(H) = H_c\delta^{0.75}P[1 - (H_c/H)] \tag{2}$$

where H_c can be expressed as

$$H_c = 0.28\delta^{-0.73} \tag{3}$$

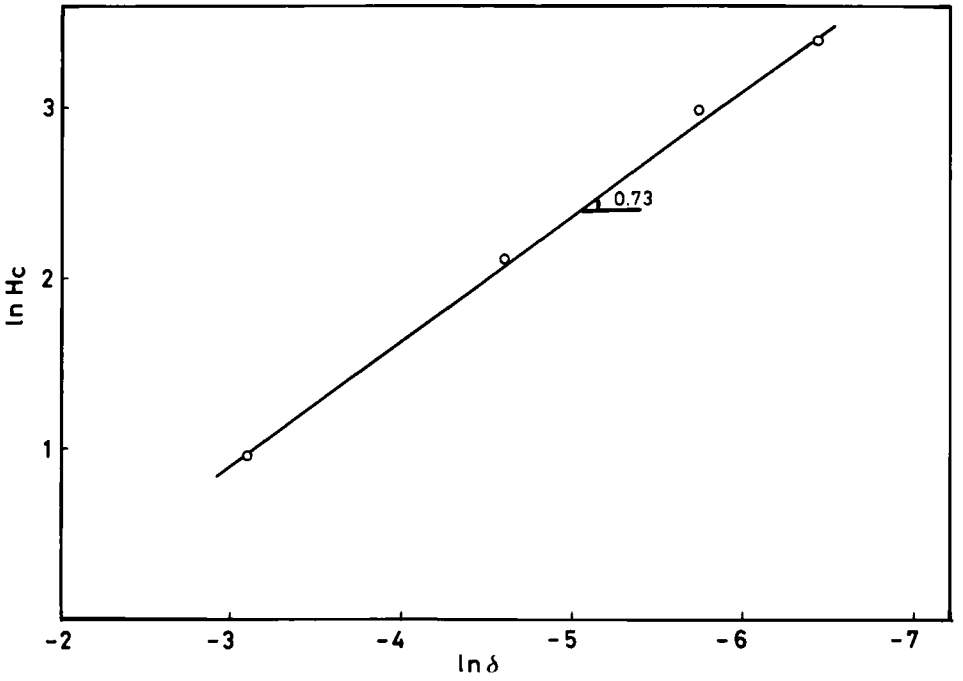

FIG. 6. Logarithmic graph of the "critical" frequency H_c vs the amplitude δ.

This relationship can be drawn by plotting mean experimental values of H_c *vs* δ (see Fig. 6).

By solving Eq. (2) for various parameters, we obtained the curves already reported in Figs. 2 and 3 (dashed lines) superimposed on the experimental ones, and made a comparison with experimental values for most of the parameters cited above.

In Table 1 the calculated values of the maximum flux allowable are compared, when possible, with the experimentally extrapolated values.

The plots of Figs. 7 and 8 report the experimental values of H_0 ("optimal frequency") as functions of oscillation amplitude δ and pressure, respectively. From the plots in these figures, H_0 values can be forecast for a wide range of vibration amplitudes and pressures.

By introducing H_0 in Eq. (2), F_0 can be calculated. By so doing, the minimal permeate fluxes necessary to assure 99.9% oil rejection can be

TABLE 1
Comparison of Experimental $F\infty$ Values (1 m^{-2}/h) with Calculated Values at Different δ and Pressure

	δ							
	0.045		0.010		0.0032		0.0016	
P	Exptl	Calcd	Exptl	Calcd	Exptl	Calcd	Exptl	Calcd
50	14	12.6	14	13.2	15	13.1	13	12.6
100	25	25.3	33	26.4	26	26.3	—	25.2
200	46	50.7	47	52.8	—	52.7	—	50.5
300	67	76	—	79.2	—	79	—	75.6
400	—	101	—	105	—	105	—	101
500	—	126	—	132	—	132	—	126
600	—	152	—	158	—	158	—	151
700	—	177	—	184	—	184	—	176
800	—	203	—	211	—	210	—	202

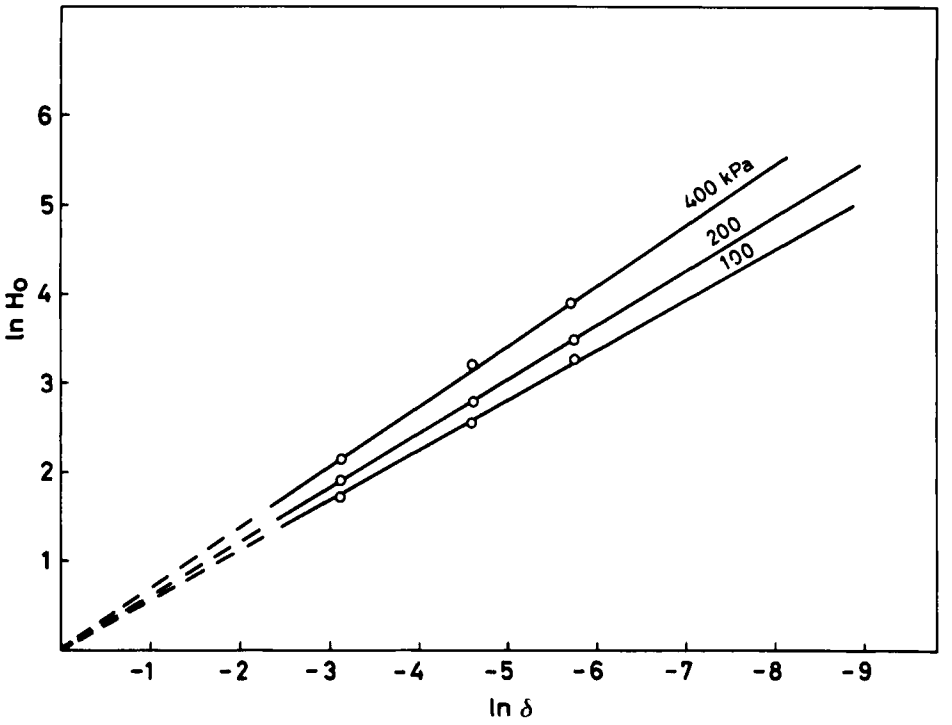

FIG. 7. Logarithmic graph of the "optimal frequency" H_0 vs the amplitude δ at different pressures.

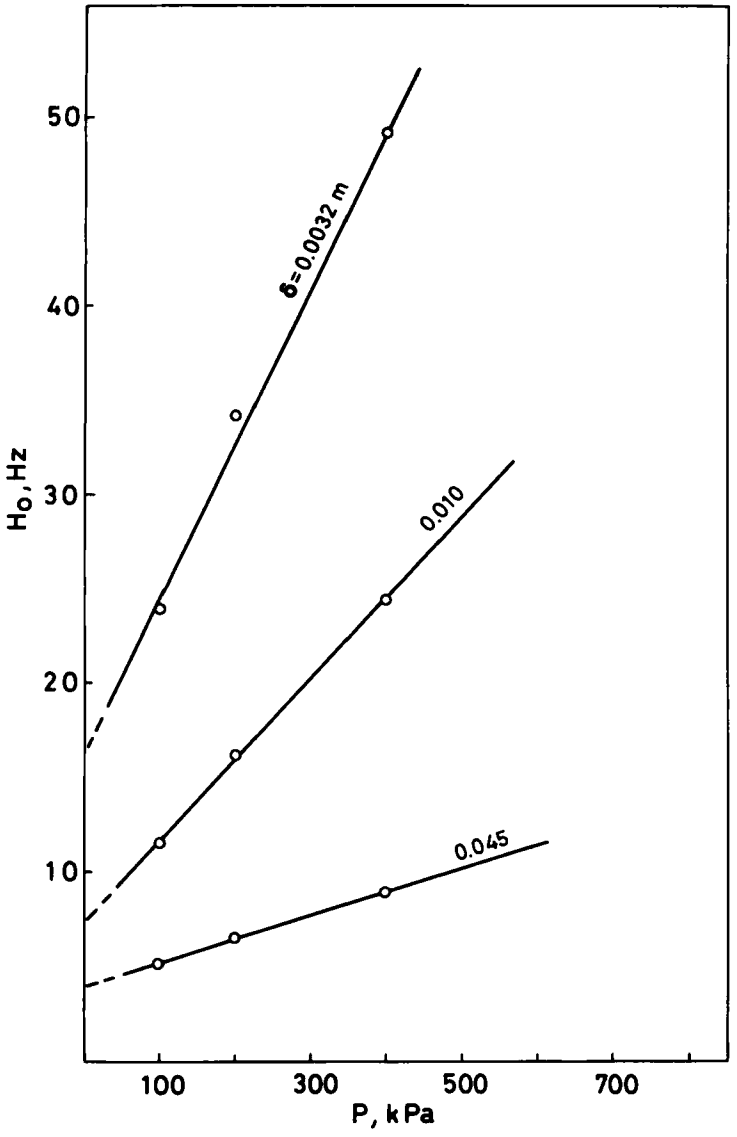

FIG. 8. Influence of the presure on the "optimal" frequency H_0 at different δ values.

TABLE 2
Comparison of Experimental F_0 Values (1 m^{-2}/h) with Calculated Values at Different δ and Pressure

	δ							
	0.045		0.010		0.0032		0.0016	
P	Exptl	Calcd	Exptl	Calcd	Exptl	Calcd	Exptl	Calcd
100	12	13.4	11.5	9.6	16	6.43	>13	4.7
200	35	32	26	25.9	23	20.5	—	19.4
400	50	72.2	39	64.9	—	62.4	—	61.2

predicted at any δ and pressure values. Some calculated F_0 are reported in Table 2 and compared, when possible with experimentally measured data.

The experimental data reported in Tables 1 and 2 seem to fit better with the calculated values at pressures lower than 300 kPa. This behavior is not surprising if account is taken of the mechanical deformation that takes place in membranes at high pressure. Compaction can occur and, consequently, apparent pore diameter reduction, which positively influences rejection but lowers permeate flux. Beyond the usual experimental uncertainty, this could explain $F\infty$ and F_0 values lower than the calculated ones.

As far as pressures lower than 100 kPa are concerned, higher fluxes are usually observed than are predicted. This behavior can be attributed to spontaneous backdiffusion of oil from the membrane surface, aided by the feeble recycle stream. This could lead to polarization layers thinner than expected; that is, to higher permeate flux.

ENERGY CONSUMPTION

As in the case of a rotating module (*3*), three kinds of energy consumption primarily contribute to different degrees to the overall power requirement for running a vibrating module:

(a) Energy necessary to feed the oil through the module.
(b) Energy spent to overcome the friction of the mechanical parts employed to generate the vibration.

(c) Energy consumed by the oscillating (membrane-bearing) part of the module.

The energy consumption of Type a (E_a) is easily calculated by taking into account the feed flux (10 times the permeate flux) and the working pressure (ranging from 50 to 800 kPa) by means of the usual relationship for pumping power evaluation. This figure ranges from 0 to 4 kWh/m^3 of permeate and thus contributes little to the total energy consumption. Energy consumption of Type b (E_b) is due to the friction of the mechanical parts listed in Fig. 1 as E (cam), R (connecting rod), N (bevel gears), and the joint connecting the driving motor. This kind of loss can be evaluated by running the module without connecting the membrane-bearing drum and measuring the electric power. We checked this, and the experimental data obtained are reported in Fig. 9 as a function of the vibration frequency.

This kind of consumption cannot be referred to the ultrafiltration volume yield because it is independent, to a first approximation, of the size of the module, provided that it has been rigorously centered on its

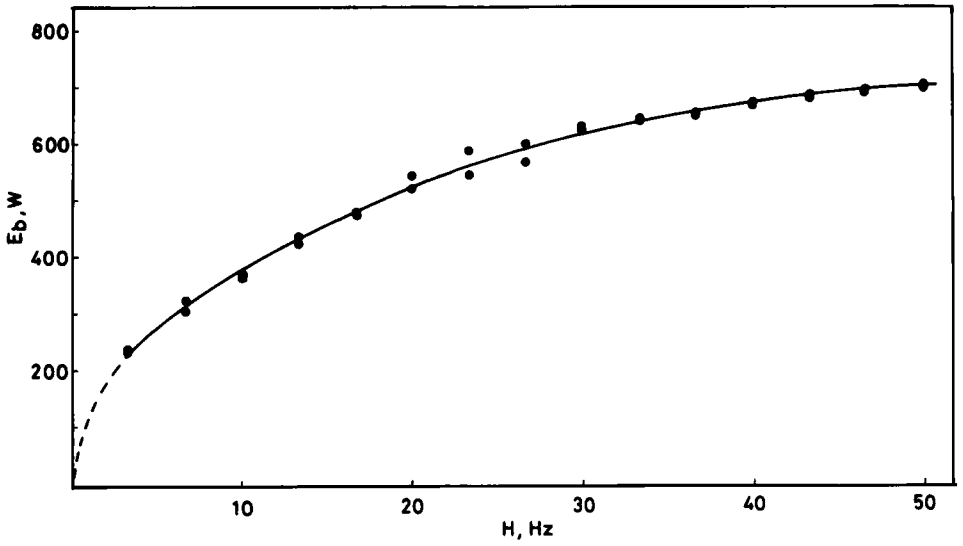

FIG. 9. Energy loss E_b as a function of frequency.

supports. For this reason E_b has been expressed as power (in watts). The trend of the plot shows that, as was to be expected, the higher the frequency, the higher the power required. The slope of the curve is the same for all the amplitude values tried and, in our opinion, is mainly influenced by the characteristics of the electric motor used.

The values reported in Fig. 9 are those used to calculate the energy consumption E_c, the net energy required to achieve the ultrafiltration of oil in our module.

Energy consumption of Type c (E_c) was evaluated by adding the E_a contribution to the measured overall consumption and then subtracting the E_b term. The result was then referred to the specific energy spent to produce 1 m^3 of permeate (kWh/m^3). Measurements and calculations were performed for each oscillation amplitude and pressure as functions of the frequency.

In Fig. 10 we reported the data obtained at different amplitudes while keeping the working pressure constant. The trends of the plots show that energy consumption reaches a maximum value near the "critical" frequency and then decreases to a value that is almost the same for all of the curves. This value does not remain constant with increasing frequency.

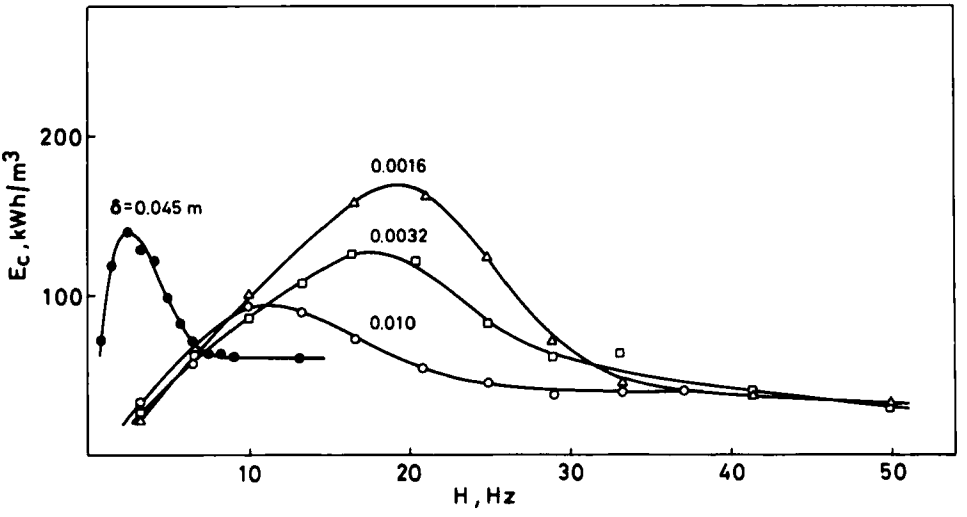

FIG. 10. Specific energy consumption E_c vs frequency at different δ values. Pressure = 200 kPa.

This behavior can easily be explained by taking into account that only in the proximity of the "critical" frequency does the permeate flux start increasing sharply (and the rejection as well). As a consequence, the energy consumption/permeate volume ratio must decrease.

Better results seem to be obtained when higher frequencies are necessary to reach the maximum permeate flux, as in the case of small oscillation amplitudes, but this could still be connected with the electrical characteristics of the motor.

More information about the influence of pressure and frequency can be obtained from the plots of Fig. 11, where E_c is reported as a function of the

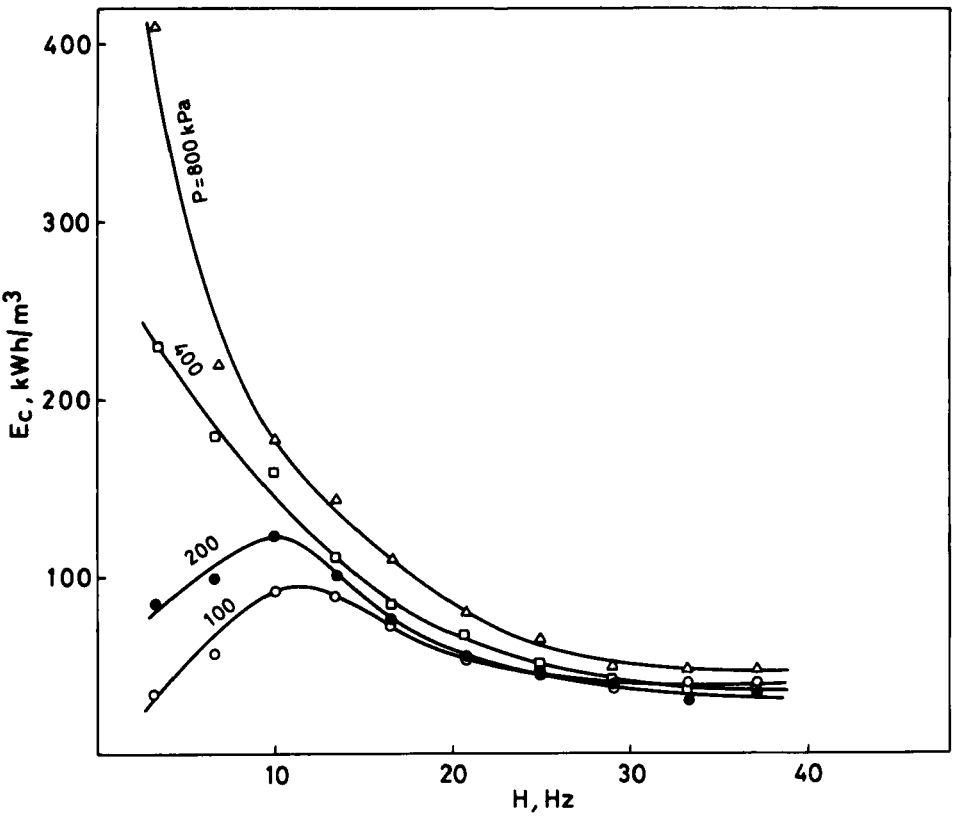

FIG. 11. Specific energy consumption E_c as a function of frequency H at different working pressures. δ = 0.010 m.

vibration frequency at 4 different working pressures. It clearly appears that the pressure negatively affects the energy required for the process at low frequency. High pressure causes an increase in friction at the mechanical seals in the module and, at the same time, facilitates a build up of the polarization layer. As a consequence, the permeate flux below the critical frequency is smaller and the energy/permeate flux ratio is increased.

It must also be noticed that the E_c value tends to increase again after reaching the already cited minimum value; this is to be expected because, while E_b regularly increases with frequency (see Fig. 9), the permeate flux tends to level at the $F\infty$ value.

The minimal energy consumption values in Table 3 are reported in Table 3. They were measured at rejections above 99.9%, that is, at frequencies above the already cited "optimal" value (H_0). This was not possible at high pressures and low amplitudes in the range of frequencies we scanned. The lowest energy values (rejection factor of less than 99.9%) are listed in parentheses. Values recorded with $\delta = 0.0016$ have a fairly high uncertainty due to the small permeate flux to be measured, and should be considered with caution. Rejection was always less than 80% in this case.

From both the graphs and the table it appears that the energy consumption per cubic meter of permeate decreases with the oscillation amplitude. This is an inverse function of pressure and frequency. Of course, the

TABLE 3
Minimal E_c and Relative Frequency H Measured at Different Amplitudes and Pressures

	δ							
	0.045		0.010		0.0032		0.0016	
P	E_c	H	E_c	H	E_c	H	E_c	H
50	150	5.8	86	10	79	41.6	(41)	41.6
100	81.6	3.2	56	29.1	36	41.6	(16)	41.6
200	60.4	13.3	37	29.1	34	50	(35)	50
300	57	13.3	30	33.3	41	50	(17)	41.6
400	48	13.3	28	33.3	(42)	50	(18)	41.6
500	41	13.3	36	33.3	(41)	50	(42)	50
600	39	13.3	36	33.3	(32)	50	(49)	50
700	38	13.3	(61)	33.3	(53)	50	(27)	41.6
800	53	11.6	(48)	33.3	(53)	50	(29)	41.6

minimal energy consumption values can be disregarded if a higher permeate production is required. In this case, higher specific costs are to be expected.

CONCLUSIONS

The experimental data obtained in this study allow us to conclude that, as expected, vibrations affect the efficiency of oil emulsion ultrafiltration. This influence can be fairly well represented by a mathematical expression which allows prediction of the behavior of the vibrating module at conditions different from the experimental ones. From the mathematical model some typical (or "critical") values can be drawn as H_c (= minimal frequency necessary to influence the process) and $F\infty$ (= maximum permeate flux attainable at the working pressure P).

Energy consumption is a function of the vibration frequency and amplitude. In our experimental conditions it ranges around the values usually measured with different kinds of traditional UF modules, although it seems to become lower with increasing vibration frequency.

Nevertheless, it must be pointed out that from the energetic point of view, our experimental module arrangement is far from being the ideal solution. In particular, unfavorable effects arise from the mechanical couplings: better energy utilization is expected from electromagnetically induced vibrations.

The influence of some important physical parameters, such as the gap width between the membrane surface and the module inner wall, and the wall roughness, is still to be investigated by us. We also plan to study the influence of high frequency and the fluid dynamic conditions at the membrane surface. Such work is in progress.

Acknowledgments

This work was partially supported by ENICHEM and Public Instruction Ministry funds. We wish to thank Mr. P. Lupino for his contribution to the mechanical parts of the experimental module.

REFERENCES

1. H. K. Lonsdale, *J. Membr. Sci., 10,* 81 (1982).
2. D. R. Lloyd, *Material Science of Synthetic Membranes,* American Chemical Society Symposium Series, Volume 269, Washington, D.C., 1985.

3. F. Vigo, C. Uliana, and P. Lupino, *Sep. Sci., Technol., 20*(2&3), 213–230 (1985).
4. F. Vigo and C. Uliana, *Ibid., 21*,(4), 367–381 (1986).
5. G. I. Taylor, *Philos. Trans. R. Soc. London, A223,* 289 (1923).
6. M. Lopez-Leiva, in *Polymer Science and Technology,* Vol. 13 (A. R. Cooper, ed.), Plenum, New York, 1980, p. 269.
7. M. Lopez-Leiva, "Ultrafiltration in Rotary Annualar Flow," PhD Thesis, Lund University, Sweden, December 1979.
8. K. Kataoka, *J. Chem. Eng. Jpn., 8*(4), 271–276 (1975).
9. R. Lemlich, *Ind. Eng. Chem., 47*(6), 1175–1180 (1955).
10. J. A. Scanlan, *Ibid., 50*(10), 1565–1568 (1958).
11. I. Raben, in *Proceedings of the 1961 Heat Transfer and Fluid Mechanics Institute* (R. C. Binder, R. L. Mannes, H. Y. Yang, and M. Epstein, eds.), 1961, pp. 90–99.
12. D. O. Barnett and R. I. Vachon, in *Heart Transfer 1970* (Fourth International Heat Transfer Conference, Paris-Versailles 1970), Vol. III, session FC 9.1.
13. I. Mamo, N. S. Orlov, Yu. I. Dytnerskii, and O. Stoch, *Vod. Gazov. Vibrosov. Fiz.-Khim. Metodami,* pp. 64–71 (1984).
14. C. C. Herrmann, *Desalination, 42,* 329–338 (1982).
15. Nitto Electric Industrial Co. Ltd., Kokai Tokkyo Koho JP 58.159.811, 22 September 1983.
16. G. Belfort, *J. Membr. Sci., 35,* 245–270 (1988).
17. R. G. Simard, *Anal. Chem., 23,* 23 (1951).

Received by editor February 15, 1989